Project Title:

Exploring on-surface photo-synthesis under ultrahigh vacuum conditions

Name:
○Chi ZHANG

Laboratory at RIKEN:
Surface and Interface Science Laboratory

---

1. Background and purpose of the project, relationship of the project with other projects

On-surface synthesis has been demonstrated as a promising bottom-up strategy to construct robust covalent nanostructures with desired patterns and efficient charge transport. Photochemical-induced covalent-bonding creation reaction (defined as "photo-synthesis" here) is highly limited on surface under ultrahigh vacuum (UHV) conditions in comparison with thermal-driven synthesis and is expected to have an increasingly broad prospect as is in conventional solution chemistry. By combination of scanning tunneling microscopy/spectroscopy (STM/STS) and density functional theory (DFT) calculations, my research has been mainly focusing on exploration of on-surface photo-synthesis under UHV conditions both experimentally and theoretically. The ultimate goal of this project is to gain deep understandings of the chemical and physical properties of adsorbates on the surface and unravel the underlying reaction mechanisms with the help of theoretical calculations.

2. Specific usage status of the system and calculation method

I have been investigating the relevant molecular systems on metal surfaces by combination of STM observations and theoretical calculations. Most of the calculations were performed in the DFT framework using the Vienna ab initio simulation package (VASP). The projector-augmented wave method was used to describe the interactions between ions and electrons. The Perdew–Burke–Ernzerhof generalized gradient approximation exchange-correlation functional was employed, and van der Waals interactions were included using the dispersion-corrected DFT-D3 method of Grimme. The atomic structures were relaxed using the conjugate gradient algorithm scheme as implemented in the VASP code until the forces on all unconstrained atoms were ≤ 0.03 eV/Å. Plane waves were used as a basis set with an energy cutoff of 400 eV. Simulated STM images were obtained based on the Tersoff–Hamann method. The climbing-image nudged elastic band (CI-NEB) was applied to locate the transition states, and the transition paths were optimized until the forces acting on the path were ≤ 0.03 eV/Å.

3. Result

In FY2023, I have systematically studied on-surface self-assembly and reactions of porphyrin-based molecules under different experimental conditions. I have successfully synthesized two kinds of Na-porphyrins by applying pure alkali metal (Na) and alkali metal salt (NaCl) on Au(111), expanding the family of metallo-porphyrins on surfaces. In addition, the construction and structural transformation of metal-organic nanostructures have also been realized based on Na and NaCl, showing the connections and differences between NaCl and Na in the structural evolutions. Accordingly, the orientation selectivity of tetrapyridyl-substituted porphyrins constrained in various molecular "Klotski puzzles" constructed from

H₂TPyP and NaCl on Au(111) has also been revealed, which provides a way to control specific molecular orientations by predesigning and constructing the corresponding local molecular environments.

(1) On-surface synthesis of Na-porphyrins [Precis. Chem. 2023, 1, 226–232]

Metallo-porphyrins with different metal centers display unique properties and are essential in various biological and chemical processes. Enormous efforts have been devoted to enriching the family of metallo-porphyrins on surfaces mainly through metalation processes within porphyrins and exogenous pure metals or intrinsic surface adatoms, which focused on transition elements. However, less attention has been paid to the synthesis of alkali-metal-based porphyrins on surface. Based on STM imaging/manipulations and DFT calculations, we report the fabrication of Na-porphyrins on Au(111) by introducing NaCl, i.e., two double-layered Na-centered porphyrins (Figure 1). Moreover, the interconversion between them was realized by precise STM manipulations.

To explore the structures of both porphyrin-based species, DFT calculations were performed. The energetically favorable structural models on Au(111) together with the corresponding STM simulations were shown in Figure 1e-j, in comparison with the high-resolution STM images of the three species (Figure 1b-d). The H₂TPyP molecule adsorbed on Au(111) adopts a saddle-shape configuration (Figure 1e), resulting in the appearance of four bright protrusions at the edges of the molecule in morphology (Figure 1b). With the absence of a metal center, the initial H₂TPyP molecule appeared with an empty black center, which was reproduced by the STM simulation (Figure 1h). As for the structures of Na-porphyrins, when two Na atoms were involved, the additional Na was located at the center of the top layer forming Na₂TPyP (Figure 1f), and a dim protrusion appeared at the molecular center in the simulated STM image (Figure 1i), in line with the

feature of a dim molecule (Figure 1c). Moreover, only when Na₅TPyP was formed (Figure 1g), could the characteristic morphology of the bright molecule (Figure 1d) be nicely reproduced by the corresponding STM simulation (Figure 1j). Moreover, the situation with the adsorption of Cl on the top of Na-porphyrin was also excluded. Accordingly, the bright molecule was attributed to Na₅TPyP, where each Na at the top layer evenly bonded to two N atoms of the porphyrin core (Figure 1g), leading to the much higher apparent height and appearance of a uniform bright protrusion.
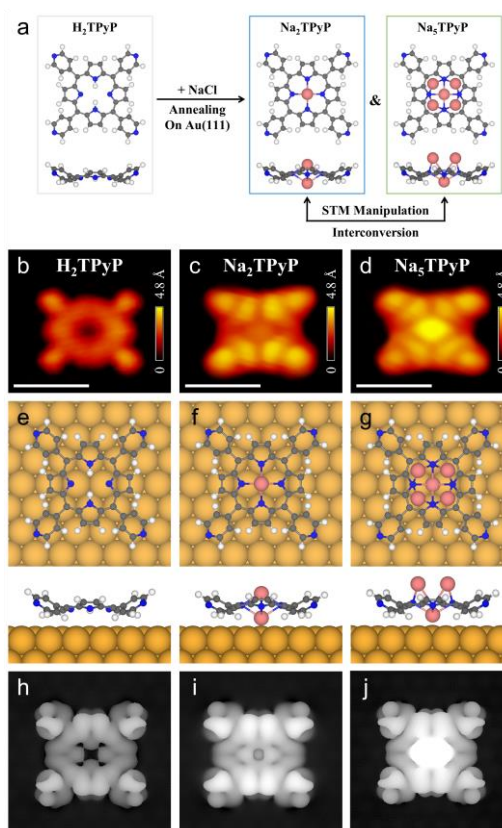

Figure 1. (a) Schematic illustration showing the fabrication of Na-porphyrins on Au(111) by introducing NaCl. (b)-(d) High-resolution STM images of (b) H₂TPyP, (c) Na₂TPyP, and (d) Na₅TPyP. Scale bar: 1 nm. (e)-(g) Top and side views of the corresponding DFT-optimized structural models on Au(111). H: white; C: gray; N: blue; Na: pink; Au: yellow. (h)-(j) Simulated STM images of (h) H₂TPyP, (i) Na₂TPyP, and (j) Na₅TPyP.

(2) Construction and structural transformation of metal-organic nanostructures based on Na and NaCl [J. Phys. Chem. Lett. 2023, 14, 3636–3642 (April,

2023)]

Metal−organic nanostructures are attractive in a variety of scientific fields, such as biomedicine, energy harvesting, and catalysis. Alkali-based metal−organic nanostructures have been extensively fabricated on surfaces based on pure alkali metals and alkali metal salts. However, their differences in the construction of alkali-based metal−organic nanostructures have been less discussed, and the influence on structural diversity remains elusive. Thus, we constructed Na-based metal−organic nanostructures by applying Na and NaCl as sources of alkali metals and visualized the structural transformations in real space. Moreover, a reverse structural transformation was achieved by dosing iodine into the Na-based metal−organic nanostructures, revealing the connections and differences between NaCl and Na in the structural evolutions.

To reveal the driving force of different structural evolutions based on NaCl and Na, we quantified the electrostatic ionic interactions involved in these structures by calculating the corresponding binding energies. The electrostatic potential maps along with the binding energies were calculated based on the optimized periodic structural models and were shown in Table 1. From the electrostatic potential maps, it can be recognized that all nitrogen atoms from pyridyl rings are negatively charged, while the Na atoms are positively charged in all these structures, which also qualitatively elaborates the electrostatic interactions as the dominant one. During Na addition, the binding energy per H_2TPyP molecule increases progressively with the Na/H_2TPyP stoichiometric ratio, from -3.64, -3.93, -4.02, to -4.18 eV/molecule. This means that by embedding more Na atoms in the molecular system, the excess Na tends to disrupt the former electrostatic interactions to form thermodynamically more favorable structures with the certain number of coexisting H_2TPyP molecules instead of existing separately, which causes the structural evolution from phase I to phase III. In contrast, when excess NaCl is supplied, the extra NaCl forms well-ordered NaCl islands with considerable ionic interactions between Na and Cl, rather than providing Na for further integration into the molecular structures. Considering the binding energy per Na, conversely, the phase transition is a thermodynamically unfavorable process for NaCl, as the binding energy within these structures decreases (from -3.64, -2.95, -2.01, to -2.09 eV/Na) during this process. Thus, after constructing phase I by consuming all the coexisting H_2TPyP molecules, Na derived from NaCl prefers to stabilize Cl as NaCl islands, instead of participating more thoroughly in the metal-organic structures while leaving the decomposed Cl alone. The competition from the ionic bonding between Na and Cl plays a crucial role in the progress of structural transformations, which determines the distinct evolution scenarios in the cases of Na and NaCl. Moreover, such evolution processes are thermodynamically driven, which is dependent on the differences in the stabilities of the corresponding structures.
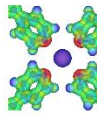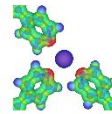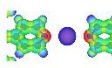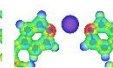

	Phase I	Intermediate phase	Phase II	Phase III
Electrostatic potential map				
Stoichiometric ratio [Na:H_2TPyP]	1:1	4:3	2:1	2:1
Binding energy [eV/molecule]	-3.64	-3.93	-4.02	-4.18
Binding energy [eV/Na]	-3.64	-2.95	-2.01	-2.09

Table 1. Electrostatic potential maps of three metal-organic phases and the corresponding binding energies involved. Red and blue colors represent negative and positive potential regions, respectively.

(3) Revelation of the orientation selectivity of tetrapyridyl-substituted porphyrins constrained in molecular "Klotski puzzles" [J. Am. Chem. Soc. 2023, 145, 22366−22373 (September, 2023)]

Understanding and controlling molecular orientations in self-assembled organic nanostructures is crucial to the development of

advanced functional nanodevices. STM provides a powerful toolbox to recognize molecular orientations and to induce orientation changes on surfaces at the single-molecule level. Enormous effort has been devoted to directly controlling molecular orientations of isolated single molecules in free space. However, revealing and further controlling molecular orientation selectivity in constrained environments remains elusive. By a combination of STM imaging/manipulations and DFT calculations, we report the orientation selectivity of tetrapyridyl-substituted porphyrins in response to various local molecular environments in artificially constructed molecular "Klotski puzzles" on Au(111). With the assistance of STM lateral manipulations, "sliding-block" molecules were able to enter predefined positions, and specific molecular orientations were adopted to fit the local molecular environments, in which the intermolecular interaction was revealed to be the key to achieving the eventual molecular orientation selectivity.

To reveal how the orientation change occurs, two possible pathways were proposed, i.e., molecular rotation and conformational change (Figure 2a). The corresponding pathways and energy barriers were calculated for two different situations, where there is (i) sufficient or (ii) constrained space for a target molecule, to interpret the cases of molecules located in a large cavity or in a 1D channel, respectively.

As for the orientation change with sufficient space, an isolated molecule adsorbed on Au(111) was applied to simplify the calculations. The energy barriers were calculated to be only ~0.05 eV for molecular rotation and ~0.91 eV for conformational change, respectively (Figure 2b), indicating that a molecule with sufficient adjacent space would tend to change its orientation via rotation. Interestingly, some asymmetric molecules with a missing leg naturally existed in the chessboard structure, which may serve as marker molecules to speculate the two possible processes experimentally based on the position of the missing part. Accordingly, in large cavities, the marker

molecules were manipulated and found to change their orientations by rotation, in line with the calculated result.

In addition, to interpret the situation of orientation change with constrained space in a 1D channel, a periodic assembled molecular structure on Au(111) was applied as a simplified system, and two pathways (i.e., molecular rotation and conformational change) were calculated (Figure 2c). Expectedly, the steric hindrance originated from the peripheral molecules significantly modifies the potential energies, and the energy barriers largely increase, which were calculated to be ~2.01 eV and ~1.65 eV for molecular rotation and con-formational change, respectively. Note that such a constraint imposed by the local molecular environment also results in a reversed order of the energy barriers of the two possible pathways compared to the case with sufficient space shown in Figure 2b. Thus, orientation change through a conformational change would be slightly preferred in this situation. While, experimentally, the orientation change of a marker molecule via conformational change or rotation was both found to be feasible.

Furthermore, the last fundamental question is when the orientation change took place, i.e., whether the manipulated molecule changed its orientation before or after diffusion. The calculated pathways in Figure 2c show that after overcoming the energy barrier of ~1.65 eV to achieve the in-situ orientation change by conformational change, the next energy barrier for the target molecule to diffuse to the adjacent position is ~1.08 eV. Accordingly, the conformational change (~1.65 eV) is the rate-determining step, when the target molecule changes its orientation before diffusion. On the other hand, if the target molecule diffuses to the next vacancy as the first step, it has to overcome the energy barrier of ~1.72 eV for diffusion and then ~1.02 eV for the in-situ orientation change through conformational change. In this case, the rate-determining step is the diffusion (~1.72 eV). Therefore, due to the similar energy barriers, the

"parking" process of a target "sliding-block" molecule may take place independent of the sequence of the orientation change and diffusion.
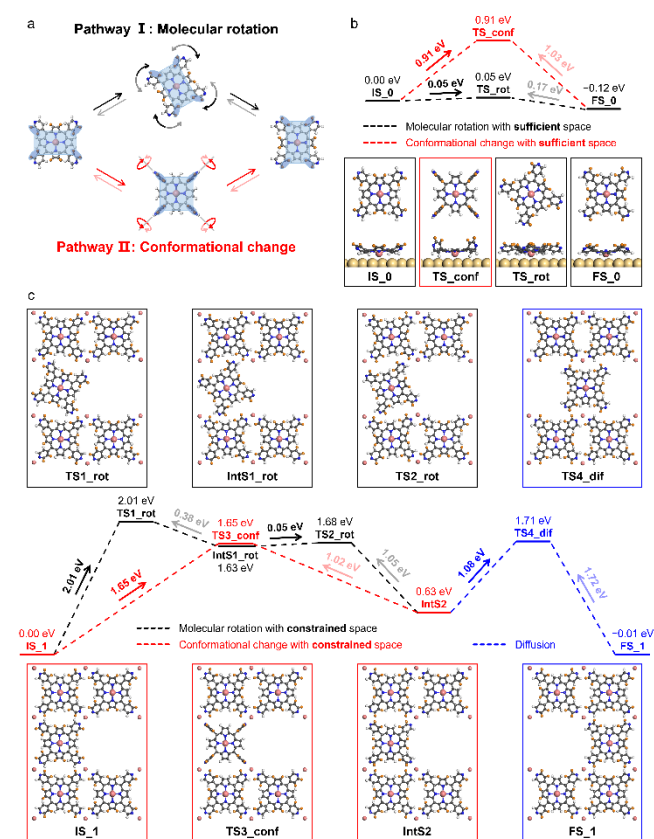

Figure 2. Two possible pathways for the orientation change of a target Na-TPyP molecule in different situations. (a) Schematic illustration showing the orientation interconversion achieved by molecular rotation and conformational change, respectively. (b) DFT-calculated pathways for the orientation change of an isolated Na-TPyP molecule (with sufficient space) adsorbed on Au(111) through molecular rotation and conformational change, respectively. (c) DFT-calculated pathways for the Na-TPyP molecules in the 1D channel (with constrained space) on Au(111) to accomplish the orientation change through molecular rotation or conformational change, followed by diffusion (as depicted by black, red, and blue dashed lines, respectively). The surfaces have been omitted for clarity. The structural models of the initial state (IS), transition state (TS), intermediate state (IntS), and final state (FS) are displayed, and their energies are provided with respect to that of the corresponding IS.

4. Conclusion

In conclusion, I have corroborated both experimentally and theoretically the metalation, self-assembly, and orientation selectivity of porphyrin-based molecules on a Au(111) surface. Our results demonstrate the feasibility of metalation by applying inorganic salt, which would serve as a promising strategy to embed intramolecular metal components into porphyrins for further functionalization and modification. In addition, visualization of the structural evolutions involving both NaCl and pure Na provide fundamental insights into the evolution of electrostatic ionic interactions and the precise fabrication of alkali-based metal−organic nanostructures. Moreover, our results also demonstrate the essential role of local molecular environments in directing single-molecule orientations, which would shed light on the design of molecular structures to control preferred orientations for further applications in molecular nanodevices.

5. Schedule and prospect for the future

In FY2024, I plan to further deeply explore some other topics related to the on-surface synthesis from the following prospects: (1) adsorption configurations; (2) molecule-molecule interactions and molecule-substrate interactions; (3) electronic and magnetic properties; (4) possible reaction pathways.

Additionally, I would like to continue using the Hokusai system for the FY2024.

Fiscal Year 2023 List of Publications Resulting from the Use of the supercomputer

[Paper accepted by a journal]

1. Zewei Yi, <u>Chi Zhang</u>*, Zhaoyu Zhang, Rujia Hou, Yuan Guo, and Wei Xu*, "On-Surface Synthesis of Na-Porphyrins Using NaCl as a Convenient Na Source" *Precis. Chem.* 2023, 1, 226–232 (April, 2023).

2. Rujia Hou, Yuan Guo, Zewei Yi, Zhaoyu Zhang, <u>Chi Zhang</u>*, and Wei Xu*, "Construction and Structural Transformation of Metal–Organic Nanostructures Induced by Alkali Metals and Alkali Metal Salts" *J. Phys. Chem. Lett.* 2023, 14, 3636–3642 (April, 2023).

3. Zewei Yi, Yuan Guo, Rujia Hou, Zhaoyu Zhang, Yuhong Gao, <u>Chi Zhang</u>*, and Wei Xu*, "Revealing the Orientation Selectivity of Tetrapyridyl-Substituted Porphyrins Constrained in Molecular "Klotski Puzzles"" *J. Am. Chem. Soc.* 2023, 145, 22366–22373 (September, 2023).

[Oral presentation]

1. <u>Chi Zhang</u>, "Study on the self-assembly, metalation, and orientation selectivity of porphyrin molecules on surface", the 9th National Conference on Surface Analytical Science and Technology Applications (NMSSA 2023), November 17-20, 2023, Fuzhou, China.